

# Brassinosteroid Biosynthesis Is Modulated via a Transcription Factor Cascade of COG1, PIF4, and PIF5<sup>1</sup>

Zhuoyun Wei, Tong Yuan, Danuše Tarkowská, Jeongsik Kim, Hong Gil Nam, Ondřej Novák, Kai He, Xiaoping Gou, and Jia Li\*

Ministry of Education Key Laboratory of Cell Activities and Stress Adaptations, School of Life Sciences, Lanzhou University, Lanzhou 730000, China (Z.W., K.H., X.G., J.L.); Department of Plant Biology and Microbiology, University of Oklahoma, Norman, Oklahoma 73019 (T.Y.); Laboratory of Growth Regulators, Centre of the Region Haná for Biotechnological and Agricultural Research, Faculty of Science, Palacký University and Institute of Experimental Botany, Academy of Sciences of the Czech Republic, CZ-78371 Olomouc, Czech Republic (D.T., O.N.); Center for Plant Aging Research, Institute for Basic Science, Daegu 42988, Republic of Korea (J.K., H.G.N.); and Department of New Biology, Daegu Gyeongbuk Institute of Science and Technology, Daegu 42988, Republic of Korea (H.G.N.)

ORCID IDs: 0000-0003-1478-1904 (D.T.); 0000-0002-8391-0258 (X.G.); 0000-0002-3148-6897 (J.L.).

Brassinosteroids (BRs) are essential phytohormones regulating various developmental and physiological processes during normal growth and development. *cog1-3D* (*cogwheel1-3D*) was identified as an activation-tagged genetic modifier of *bri1-5*, an intermediate BR receptor mutant in *Arabidopsis* (*Arabidopsis thaliana*). *COG1* encodes a Dof-type transcription factor found previously to act as a negative regulator of the phytochrome signaling pathway. *cog1-3D* single mutants show an elongated hypocotyl phenotype under light conditions. A loss-of-function mutant or inducible expression of a dominant negative form of *COG1* in the wild type results in an opposite phenotype. A BR profile assay indicated that BR levels are elevated in *cog1-3D* seedlings. Quantitative reverse transcription-polymerase chain reaction analyses showed that several key BR biosynthetic genes are significantly up-regulated in *cog1-3D* compared with those of the wild type. Two basic helix-loop-helix transcription factors, *PIF4* and *PIF5*, were found to be transcriptionally up-regulated in *cog1-3D*. Genetic analysis indicated that *PIF4* and *PIF5* were required for *COG1* to promote BR biosynthesis and hypocotyl elongation. Chromatin immunoprecipitation and electrophoretic mobility shift assays indicated that *COG1* binds to the promoter regions of *PIF4* and *PIF5*, and *PIF4* and *PIF5* bind to the promoter regions of key BR biosynthetic genes, such as *DWF4* and *BR6ox2*, to directly promote their expression. These results demonstrated that *COG1* regulates BR biosynthesis via up-regulating the transcription of *PIF4* and *PIF5*.

Brassinosteroids (BRs) are a class of naturally occurring hormone mediating multiple developmental and physiological processes during normal growth and

development, such as photomorphogenesis, vascular differentiation, senescence, cell elongation, and cell division and differentiation (Clouse and Sasse, 1998). Within the last four decades, BR biosynthesis, catabolism, and signal transduction pathways have been largely elucidated. It is known that brassinolide (BL), the final product of the BR biosynthetic pathway and the most active BR, can directly interact with the extracellular domain of a Leu-rich repeat receptor-like kinase (LRR-RLK), BRASSINOSTEROID-INSENSITIVE1 (BRI1; Kinoshita et al., 2005; Hothorn et al., 2011; She et al., 2011). BL binding to BRI1 causes the release of BRI1 KINASE INHIBITOR1 from BRI1, allowing BRI1-BL to associate with a second LRR-RLK named BRI1-ASSOCIATED RECEPTOR KINASE1 (BAK1; Li et al., 2002; Nam and Li, 2002; Wang and Chory, 2006; Jaillais et al., 2011). Structure analyses revealed that BL is directly involved in the interaction of the BRI1-BL complex with BAK1, which is consistent with genetic data showing that BAK1 is essential for the early events of the BR signaling pathway (Gou et al., 2012; He et al., 2013; Santiago et al., 2013; Sun et al., 2013). The perception of BL at the cell surface by BRI1/BAK1 initiates a reversible phosphorylation and

<sup>1</sup> This work was supported by the National Natural Science Foundation of China (grant nos. 31530005, 31470380, and 91317311 to J.L.), the Ministry of Education (2011 Scholarship Award for Excellent Doctoral Student to Z.W.), the China Postdoctoral Science Foundation (grant no. 2016M602889 to Z.W.), the Ministry of Agriculture of the People's Republic of China (grant no. 2016ZX08009-003-002 to K.H.), the Návrat program from the Ministry of Education, Youth, and Sports of the Czech Republic (grant no. LK21306 to O.N.), the Czech Science Foundation (grant no. GA14-34792S to O.N.), and the Institute for Basic Science (grant no. IBS-R013-D1 to H.G.N.).

\* Address correspondence to [lijia@lzu.edu.cn](mailto:lijia@lzu.edu.cn).

The author responsible for distribution of materials integral to the findings presented in this article in accordance with the policy described in the Instructions for Authors ([www.plantphysiol.org](http://www.plantphysiol.org)) is: Jia Li ([lijia@lzu.edu.cn](mailto:lijia@lzu.edu.cn)).

Z.W., X.G., and J.L. conceived the original screening and research plans; J.L. supervised the experiments; Z.W. performed most of the experiments; T.Y., D.T., and J.K. performed some of the experiments; Z.W., X.G., K.H., D.T., J.K., H.G.N., O.N., and J.L. analyzed the data; Z.W. and J.L. wrote the article.

[www.plantphysiol.org/cgi/doi/10.1104/pp.16.01778](http://www.plantphysiol.org/cgi/doi/10.1104/pp.16.01778)

dephosphorylation cascade, leading to the dephosphorylation and inactivation of an important negative regulator, BRASSINOSTEROID-INSENSITIVE2 (BIN2), a GSK3-like kinase (Li and Nam, 2002; Mora-García et al., 2004; Kim et al., 2009, 2011). Without early BR signaling, BIN2 phosphorylates BRASSINAZOLE-RESISTANT1 (BZR1) and BRI1-EMS-SUPPRESSOR1 (BES1) to trigger their destruction (Wang et al., 2002b; Yin et al., 2002). Recent studies revealed that BIN2 has additional substrates that modulate downstream BR signaling. One of them is PHYTOCHROME INTERACTING FACTOR4 (PIF4), a basic helix-loop-helix transcription factor mainly regulating cell elongation (Castillon et al., 2007; de Lucas et al., 2008; Oh et al., 2012). BIN2 phosphorylates PIF4, leading this transcriptional regulator to a proteasome-mediated degradation process, which plays a prevalent role in timing hypocotyl elongation to late night (Bernardo-García et al., 2014). When BR signaling is induced, BIN2 is inactivated, and BZR1/BES1 and PIF4 are rapidly dephosphorylated and subsequently move into the nucleus to form a transcription factor complex synergistically activating a common set of BR-regulated genes involved in diverse processes of plant growth and development (He et al., 2002; Wang et al., 2002b; Yin et al., 2002; Sun et al., 2010; Yu et al., 2011; Oh et al., 2012).

The main BR biosynthetic pathway has also largely been elucidated (Zhao and Li, 2012). Campesterol is thought to be the first precursor entering into the specific BR biosynthetic pathway. Campesterol is converted to campestanol through a C-22 oxidation pathway. Campestanol is then converted to castasterone (CS) via an early or a late C-6 oxidation pathway (Suzuki et al., 1994a, 1994b; Fujioka et al., 1995; Choi et al., 1996, 1997). CS is ultimately converted to BL (Yokota et al., 1990; Suzuki et al., 1993). Both CS and BL are active BRs, with CS showing only about 10% of the activity of BL (Kinoshita et al., 2005). Until now, more than 70 BRs have been identified in plants (Fujioka and Yokota, 2003; Bajguz, 2007). Catalytic activities of several BR biosynthetic enzymes, such as DEETIOLATED2 (DET2), CONSTITUTIVE PHOTOMORPHOGENESIS AND DWARFISM (CPD), ROTUNDIFOLIA3 (ROT3), CYP90D1, DWARF4 (DWF4), BRASSINOSTEROID-6-OXIDASE1 (BR6ox1), and BR6ox2, have been elucidated. For example, DET2 catalyzes 5 $\alpha$  reduction steps of the early BR biosynthetic pathway (Li et al., 1996; Fujioka et al., 1997, 2002; Noguchi et al., 1999b). CPD is involved in the C-3 oxidation steps of BR biosynthesis (Ohnishi et al., 2012). DWF4 encodes a C-22 hydroxylase that catalyzes the C-22 hydroxylation of multiple BR biosynthesis intermediates (Choe et al., 1998; Fujita et al., 2006). ROT3, also known as CYP90C1, and its homolog CYP90D1 are essential enzymes for the C-23 hydroxylation steps (Ohnishi et al., 2006). BR6ox1 and BR6ox2 catalyze multiple C-6 oxidation reactions connecting the early and late C-6 oxidation pathways. In addition, BR6ox2 participates in a final biosynthetic step, converting CS to BL (Bishop et al., 1999; Shimada et al., 2001; Kim et al., 2005).

Mutants impaired in BR biosynthesis show a severely retarded growth phenotype, whereas application of an excessive amount of BRs also inhibits root growth, suggesting that BR homeostasis is critical for optimal growth and development (Chory et al., 1991; Szekeres et al., 1996; Choe et al., 1998; Clouse and Sasse, 1998). Plants developed several strategies to tightly control endogenous BR levels. For example, the expression of many BR biosynthetic genes is negatively feedback controlled by the BR signaling pathway (Mathur et al., 1998; Bancoş et al., 2002). Activated BZR1 and BES1 can repress the expression of *CPD* and *DWF4* by directly binding to their promoters when BR signaling is strong enough to maintain normal plant growth and development (He et al., 2005; Sun et al., 2010; Yu et al., 2011). Plants also can accelerate the BR biosynthetic rate to quickly produce more BRs when needed for certain developmental stages or environmental conditions. TEOSINTE BRANCHED1/CYCLOIDEA/PROLIFERATING CELL FACTOR1 (TCP1) and CESTA (CES) can up-regulate the expression of *DWF4* and *CPD* by associating with the conserved motifs in their respective promoters (Guo et al., 2010; Poppenberger et al., 2011; Gao et al., 2015). Auxin or high temperature also can induce *DWF4* expression (Chung et al., 2011; Maharjan and Choe, 2011). However, the detailed mechanisms controlling BR biosynthesis by environmental cues are poorly understood.

To identify additional regulators mediating BR biosynthesis, we carried out a large-scale genetic screen in an intermediate mutant of the BR receptor named *bri1-5*. A number of *bri1-5* genetic modifiers have been isolated (Li et al., 2001, 2002; Zhou et al., 2004; Yuan et al., 2007; Guo et al., 2010). One of these mutants is *cog1-3D* (*cogwheel1-3D*). *COG1* encodes a Dof-type transcription factor that is involved in phytochrome signaling and seed tolerance to deterioration (Park et al., 2003; Bueso et al., 2016). In this report, we provide strong evidence to show that *COG1* can directly up-regulate the expression of *PIF4* and *PIF5* by associating with their promoter regions. *PIF4* and *PIF5* bind to the promoters of *DWF4* and *BR6ox2* to directly enhance their expression. Our analyses revealed that *PIF4* and *PIF5* are key regulators mediating BR biosynthesis, demonstrating that light signaling is critical to BR homeostasis.

## RESULTS

### *cog1-3D* Partially Suppresses the Short-Hypocotyl Phenotype of *bri1-5*

To identify additional components regulating BR signaling or homeostasis, we generated a large-scale activation-tagging pool in a weak *bri1* allele, *bri1-5*, using a *pBIB-BASTA-AT2* vector as described previously (Gou and Li, 2012). From about 120,000 transgenic plants, an extragenic suppressor was identified with significantly elongated hypocotyls compared with *bri1-5* (Fig. 1, A and B). Scanning electron microscopy analysis indicated that the longer hypocotyls of the

double mutants are caused mainly by elongated cells (Fig. 1, C and D). Genetic analysis indicated that the mutant phenotype is controlled by a dominant gene that cosegregates with the herbicide-resistant gene from the T-DNA of the activation-tagging construct.

To clone the gene responsible for the elongated hypocotyl phenotype, we backcrossed the double mutant with WS2, and the *bri1-5* mutation was segregated out. The single mutants exhibit significantly longer hypocotyls than those of WS2 (Fig. 2A). Thermal asymmetry interlaced PCR was used to amplify the genomic sequences flanking the T-DNA insertion site (Liu and Whittier, 1995). Sequence analysis indicated that the T-DNA was inserted 1,400 bp upstream of the translation initiation codon of *COG1* (At1g29160; Fig. 2B). The suppressor was named *cog1-3D*, as two dominant alleles, *cog1-D* and *cog1-2D*, were reported previously (Park et al., 2003; Bueso et al., 2016). To further determine whether *COG1* is the gene responsible for the longer hypocotyl phenotype, transgenic plants harboring *35S:FLAG-COG1* were generated. Among 50 total transgenic plants obtained, over 90% of them showed elongated hypocotyl phenotypes, similar to that of the *cog1-3D* single mutant (Fig. 2, A and C). Real-time reverse transcription (RT)-PCR analysis confirmed that *COG1* is indeed overexpressed in both the activation-tagged mutants and the *35S:FLAG-COG1* transgenic lines (Fig. 2D). These results confirmed that elevated expression of *COG1* is the main cause of the longer hypocotyl phenotypes of the activation-tagged line.

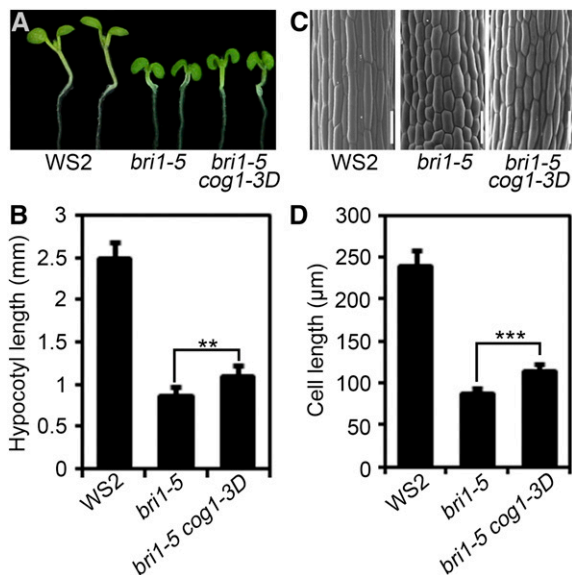


**Figure 1.** *cog1-3D* partially suppresses the short hypocotyl phenotype of *bri1-5*. A, Phenotypes of WS2, *bri1-5*, and *bri1-5 cog1-3D* seedlings. B, Hypocotyl lengths of the seedlings shown in A. C, Scanning electron micrographs showing that *cog1-3D* partially suppresses the short hypocotyl cell length phenotype of *bri1-5*. Middle parts of the hypocotyls were used for the scanning analyses. Bars = 150 µm. D, Cell lengths of *bri1-5* and *bri1-5 cog1-3D* hypocotyls shown in C.

### Loss of Function by Ethyl Methanesulfonate Point Mutation or Inducible Expression of the *COG1-SRDX* Chimeric Gene Results in a Short-Hypocotyl Phenotype

To further determine whether the function of *COG1* is required for hypocotyl elongation, loss-of-function mutants of *COG1* were searched from various resources. No T-DNA insertion alleles were identified from available databases. A *cog1-6* mutant was identified as an intragenic suppressor of *cog1-D*, the first activation-tagged allele of *COG1* (Park et al., 2003), from a large-scale ethyl methanesulfonate-mutagenized screen. The *cog1-6* mutant contains a deletion of a single G at position 85, resulting in a premature stop codon (Fig. 2B). The *cog1-6* mutation caused a significant inhibition of the long-hypocotyl phenotype of *cog1-D* and a slightly reduced hypocotyl length compared with that of wild-type seedlings, especially under red light (Fig. 2, E and F; Supplemental Fig. S1).

The subtle developmental phenotypes observed in *cog1-6* plants suggested that homologs of *COG1* may play redundant roles with *COG1*. As a matter of fact, phylogenetic analysis revealed that a number of proteins are closely related to *COG1* (Yanagisawa, 2002). Therefore, we employed a dominant negative technology, named chimeric repressor gene silencing, to further examine the roles of *COG1* and its homologs. This technology has been used successfully to determine the roles of numerous functionally redundant transcription factors (Hiratsu et al., 2003; Guo et al., 2010; Poppenberger et al., 2011). *COG1* was fused with an EAR repressor domain (*SRDX*), and the chimeric version should effectively repress the expression of the target genes of *COG1* and its redundant proteins. Since constitutive expression of *COG1-SRDX* driven by the *35S* promoter resulted in a seedling lethality phenotype (Supplemental Fig. S2), we made a dexamethasone (DEX)-inducible *COG1-SRDX* construct (*GVG:COG1-SRDX*) and generated corresponding transgenic plants (Aoyama and Chua, 1997). Homozygous lines for the transgene were selected and examined for the hypocotyl growth phenotype with or without DEX treatment. When 2-d-old seedlings from one-half-strength Murashige and Skoog (MS) medium were transferred to the medium containing DEX and grown for an additional 5 d, the *GVG:COG1-SRDX* transgenic seedlings showed significantly shortened hypocotyls due to reduced cell length (Fig. 2, G and H; Supplemental Fig. S3), which is similar to the *cog1-6* mutant and the *COG1* antisense seedlings (Fig. 2, E and F; Park et al., 2003). Without DEX treatment, the transgenic plants show no defective phenotypes compared with the wild type (Fig. 2, G and H; Supplemental Fig. S3). Nontransgenic plants grown on one-half-strength MS medium with or without DEX treatment did not show any altered phenotypes, confirming that the shortened hypocotyl phenotype was indeed caused by induced expression of *COG1-SRDX*. These results demonstrated that *COG1* plays an important role in hypocotyl elongation.

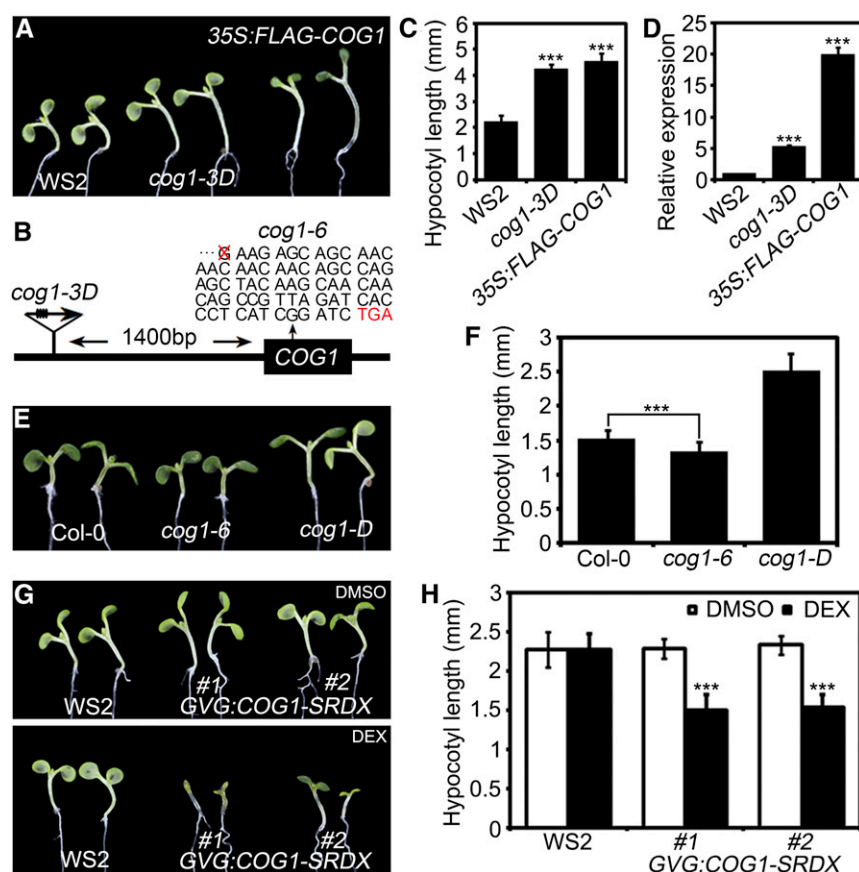


**Figure 2.** COG1 plays an important role in regulating hypocotyl elongation. A, Phenotypes of WS2, *cog1-3D*, and 35S:FLAG-COG1 seedlings. B, In *cog1-3D*, a T-DNA fragment from the activation-tagging construct *pBIB-BASTA-AT2* was inserted at 1,400 bp upstream of the start codon of *COG1* (At1g29160). The *cog1-6* mutant contains a deletion of a single G at position 85 bp, resulting in a premature stop codon after amino acid 51. C, Hypocotyl measurements of the seedlings shown in A. D, Real-time RT-PCR assay indicated that the expression of *COG1* was elevated in both *cog1-3D* and 35S:FLAG-COG1 seedlings. E, Phenotypes of Columbia-0 (Col-0), *cog1-6*, and *cog1-D* seedlings grown under long-day conditions. F, Hypocotyl lengths of the seedlings shown in E. G, Induced expression of a dominant negative chimeric gene, *COG1-SRDX*, inhibits hypocotyl elongation. Wild-type and *GVG:COG1-SRDX* transgenic seedlings were germinated on one-half-strength MS medium plates for 2 d and then transferred to one-half-strength MS medium supplemented with mock solution (dimethyl sulfoxide [DMSO]; top) or 10  $\mu$ M DEX (bottom) for an additional 5 d. H, Hypocotyl lengths of the seedlings shown in G.

### The *cog1-3D* Seedlings Are Insensitive to Exogenously Applied BRs Due to Elevated Endogenous BR Levels

COG1 partially suppressing the short-hypocotyl phenotype of *bri1-5* suggests that COG1 is involved in BR-related pathways. To investigate how COG1 regulates BR-related pathways, we first examined the effect of 24-epibrassinolide (24-epiBL) on the hypocotyl growth of *cog1-3D*. The hypocotyl growth of WS2 is promoted by exogenously applied different concentrations of 24-epiBL ranging from 1 to 1,000 nM (Fig. 3A). The hypocotyl growth of *cog1-3D* mutants, however, is insensitive to exogenously supplied different concentrations of 24-epiBL (Fig. 3A).

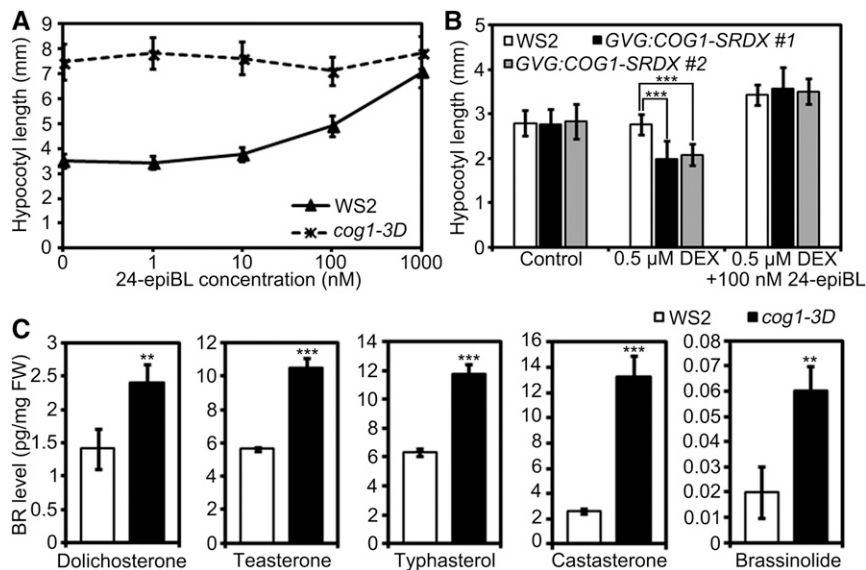
Either blocking the BR signaling pathway or increasing endogenous levels of BRs can result in plant insensitivity to exogenous BRs. The fact that *cog1-3D* shows an elongated but not a shortened hypocotyl phenotype suggests the BR signaling is at least not blocked in *cog1-3D*. The phosphorylation status of BES1 was investigated with a specific anti-BES1 antibody in wild-type and *cog1-3D* seedlings after treatment with or without 1  $\mu$ M 24-epiBL (Yin et al., 2002). Interestingly, the levels of both phosphorylated and unphosphorylated BES1 in *cog1-3D* mutants were higher than those of wild-type seedlings without BR treatment (Supplemental Fig. S4A). Upon BR treatment, unphosphorylated BES1 was increased dramatically, and phosphorylated BES1

disappeared in both wild-type and mutant seedlings. The amount of unphosphorylated BES1 in *cog1-3D* also was greater than that of wild-type seedlings (Supplemental Fig. S4A). Consistently, the expression of a BR signaling marker gene, *SAUR-AC1*, was increased significantly in *cog1-3D* plants (Supplemental Fig. S4B). These results confirmed that BR signaling is enhanced in *cog1-3D* plants.

Next, we investigated whether the endogenous levels of BRs are elevated in *cog1-3D*. If COG1 promotes BR biosynthesis, the shortened hypocotyl phenotype of *COG1-SRDX* should result from the reduced BR biosynthesis and the phenotype should be rescued by exogenously applied BRs. Indeed, the shortened hypocotyl phenotype of *GVG:COG1-SRDX* plants grown on medium containing DEX was rescued by supplying 100 nM 24-epiBL in the medium (Fig. 3B). In addition, blocking BR biosynthesis using a specific inhibitor, brassinazole (BRZ), should shorten the hypocotyls of *cog1-3D* plants (Asami et al., 2000). Indeed, the *cog1-3D* seedlings exhibited a hypocotyl length indistinguishable from that of wild-type controls when grown on one-half-strength MS medium agar plates supplied with 1  $\mu$ M BRZ (Supplemental Fig. S5). These results support the hypothesis that COG1 promotes hypocotyl elongation by increasing endogenous BR levels.

BR profile analysis was performed using WS2 and *cog1-3D* seedlings. It is apparent that BL, CS, and

**Figure 3.** The *cog1-3D* seedlings showed reduced sensitivity to BR due to increased endogenous BR amounts. A, Hypocotyl growth analyses of 7-d-old *cog1-3D* and wild-type seedlings grown on one-half-strength MS agar plates containing different concentrations of 24-epiBL. B, The shortened hypocotyl phenotype of *COG1-SRDX* can be rescued by exogenous 24-epiBL application. WS2 and *GVG:COG1-SRDX* seedlings were grown on one-half-strength MS medium with or without 0.5  $\mu\text{M}$  DEX or with 0.5  $\mu\text{M}$  DEX and 100 nM 24-epiBL for 6 d. C, Endogenous BR levels in *cog1-3D* and wild-type plants. The data shown are averages and SD from three independent replicates. FW, Fresh weight.



several of their precursors are significantly elevated in *cog1-3D* seedlings (Fig. 3C). For example, dolichosterone, teasterone and typhasterol are increased by approximately 2-fold in *cog1-3D* seedlings compared with the wild type; CS is elevated by about 5-fold in *cog1-3D*; BL is increased by 3-fold in *cog1-3D* seedlings (Fig. 3C). These results suggested that COG1 possibly enhances BR biosynthesis by affecting multiple reactions in the biosynthesis pathway. Alternatively, it is also possible that BR catabolism is decreased in *cog1-3D*.

### COG1 Up-Regulates the Expression of BR Biosynthetic Genes

To examine whether BR biosynthesis is enhanced or BR catabolism is decreased in *cog1-3D*, we compared the expression levels of all known key genes involved in both BR biosynthesis and catabolism from *cog1-3D* and wild-type seedlings. The transcript levels of *DET2*, *CYP90D1*, and *BR6ox1* in *cog1-3D* showed no significant differences from those of the wild type (Supplemental Fig. S6), whereas the expression levels of *CPD*, *DWF4*, *ROT3*, and *BR6ox2* are significantly up-regulated in *cog1-3D* and *35S:FLAG-COG1* compared with wild-type seedlings (Fig. 4A). Consistently, inducible expression of *COG1-SRDX* resulted in the down-regulation of these four genes (Fig. 4B). All the catabolism genes are not significantly down-regulated in *cog1-3D* compared with those in wild-type seedlings. Several of the catabolic genes are actually up-regulated in *cog1-3D* (Supplemental Fig. S7). These results suggested that BR accumulation in *cog1-3D* is caused mainly by enhanced BR biosynthesis rather than by decreased BR catabolism.

To further investigate whether COG1 promoting hypocotyl elongation relies on BR biosynthesis, *cog1-3D* plants were crossed with various mutants deficient in BR biosynthesis. The homozygous *det2 cog1-3D*, *cpd*

*cog1-3D*, *dwf4 cog1-3D*, and *br6ox1 br6ox2 cog1-3D* mutants were obtained and examined for their hypocotyl growth phenotypes. All these double or triple mutants show hypocotyl elongation phenotypes indistinguishable from the corresponding single or double mutants (Fig. 4, C and D). Furthermore, deficiency in BR signal transduction also completely inhibits the hypocotyl elongation of *cog1-3D* (Supplemental Fig. S8). These results clearly indicated that COG1 regulation of hypocotyl elongation depends on BR biosynthesis and signaling.

### PIF4 and PIF5 Are Up-Regulated by COG1 and Are Required for COG1-Mediated BR Biosynthesis and Hypocotyl Elongation

Although the expression of *CPD*, *DWF4*, *ROT3*, and *BR6ox2* is transcriptionally regulated by COG1, we failed to detect the direct association of COG1 with their promoters by chromatin immunoprecipitation (ChIP) analyses, indicating that COG1 regulates the expression of these genes possibly via other unknown transcription factors. An RNA sequencing analysis was performed to compare the expression profiles of WS2 and *cog1-3D*. We identified a total of 443 genes displaying statistically significant 2-fold expression changes in *cog1-3D* compared with wild-type seedlings, including 37 transcription factors (Supplemental Table S1). PIF4 and PIF5 are among those 37 transcription factors. PIF4 and PIF5 play a pivotal role in cell elongation by directly elevating the expression of genes involved in cell wall loosening (Huq and Quail, 2002; de Lucas et al., 2008; Oh et al., 2012; Supplemental Fig. S9). To investigate whether PIF4 and PIF5 are involved in COG1-mediated hypocotyl elongation, the expression of *PIF4* and *PIF5* in *cog1-3D* and wild-type plants was confirmed using real-time RT-PCR. Both *PIF4* and *PIF5* are up-regulated in *cog1-3D* as well as *35S:FLAG-COG1*

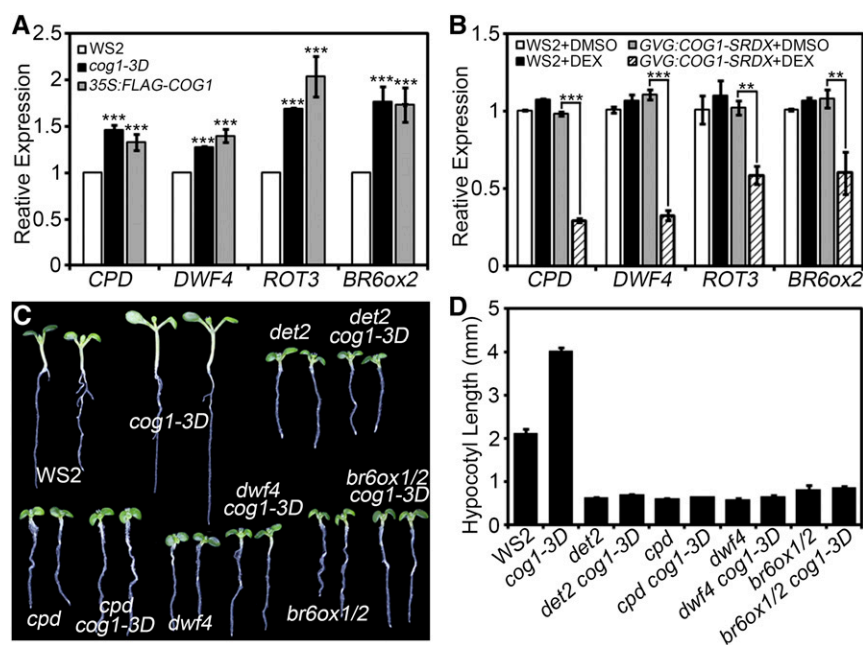


**Figure 4.** COG1 up-regulates the expression of BR biosynthetic genes, and COG1 regulation of hypocotyl elongation is dependent on BR biosynthesis. A, Expression levels of *CPD*, *DWF4*, *ROT3*, and *BR6ox2* in WS2, *cog1-3D*, and 35S:FLAG-COG1 plants were detected by quantitative reverse transcription (qRT)-PCR. B, Expression levels of *CPD*, *DWF4*, *ROT3*, and *BR6ox2* in WS2 and GVG:COG1-SRDX transgenic plants with or without DEX treatment. WS2 and GVG:COG1-SRDX seedlings were treated with mock solution (DMSO) or 10  $\mu$ M DEX for 24 h before harvest for RNA extraction and qRT-PCR analyses. C, *cog1-3D* showed no or less effect on hypocotyl elongation in various BR biosynthetic mutants. One-week-old seedlings of WS2, *cog1-3D*, *det2*, *det2 cog1-3D*, *cpd*, *cpd cog1-3D*, *dwf4*, *dwf4 cog1-3D*, *br6ox1 br6ox2*, and *br6ox1 br6ox2 cog1-3D* are shown. D, Hypocotyl lengths of the seedlings shown in C.

seedlings compared with wild-type plants (Fig. 5A). To investigate whether the protein levels of PIF4 and PIF5 also are accumulated, we performed western-blot analysis. Consistently, the protein level of PIF5 is increased significantly in *cog1-3D* and 35S:FLAG-COG1 seedlings (Supplemental Fig. S10). PIF4 levels in *cog1-3D* and 35S:FLAG-COG1 were not examined due to unavailable specific antibody against PIF4. Inducible expression of COG1-SRDX, on the other hand, resulted in significantly decreased expression of PIF4 and PIF5 (Fig. 5B).

To further determine whether PIF4 and PIF5 are essential for COG1-mediated cell elongation, *cog1-3D* plants were crossed with *pif4* and *pif5* single and *pif4 pif5* double mutants. The *pif4 cog1-3D* and *pif5 cog1-3D* seedlings exhibited partially inhibited hypocotyl elongation compared with the *cog1-3D* single mutant (Fig. 5, C and D), whereas *pif4 pif5 cog1-3D* triple mutant seedlings showed hypocotyl length almost identical to that of the *pif4 pif5* double mutants (Fig. 5, C and D). Plants grown under continuous red light showed similar results (Supplemental Fig. S11). In addition, the expression levels of *CPD*, *DWF4*, *ROT3*, and *BR6ox2* in *pif4 pif5 cog1-3D* triple mutants showed no significant differences from *pif4 pif5* double mutants (Fig. 5E). These results suggested that the function of COG1 in regulating BR biosynthesis and hypocotyl elongation is dependent on PIF4 and PIF5.

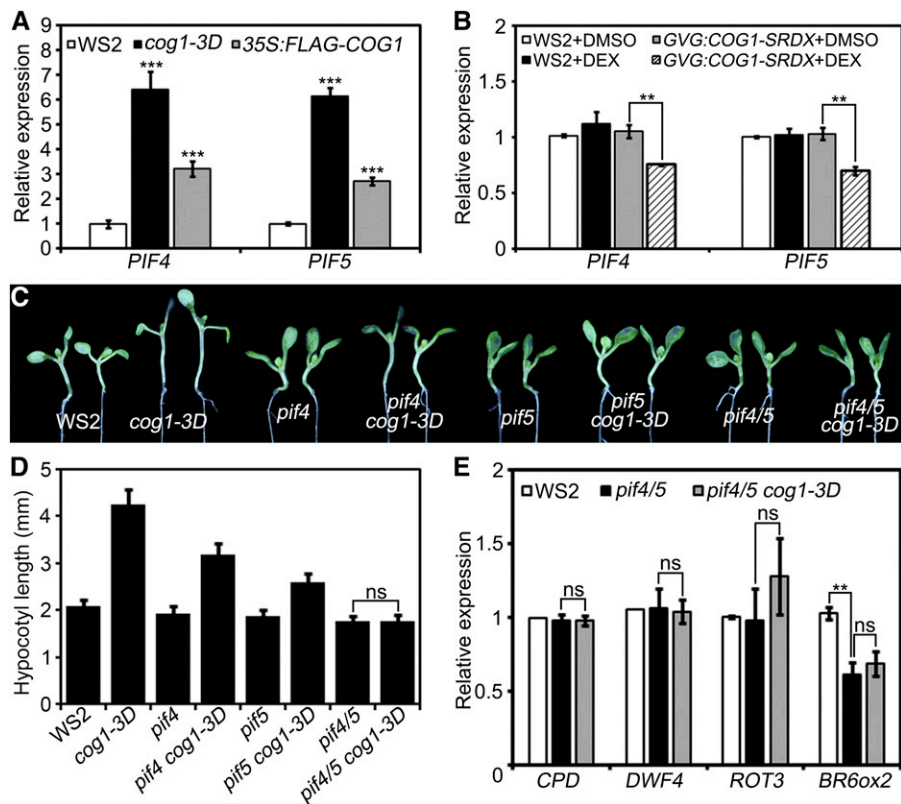
#### COG1 Binds Directly to the Promoters of PIF4 and PIF5

Since PIF4 and PIF5 are transcriptionally regulated by COG1 in plants and the function of COG1 is dependent on PIF4 and PIF5 (Fig. 5), we hypothesized that COG1 may directly regulate the expression of PIF4 and

PIF5. To test this hypothesis, COG1 was fused with a hormone-binding domain of a human estrogen receptor (ER) at its C terminus, and transgenic plants harboring the chimeric gene driven by a 35S promoter (35S:COG1-ER) were generated. Six-day-old transgenic seedlings were pretreated with 10  $\mu$ M cycloheximide (CHX) for 2 h to prevent the biosynthesis of new proteins. Estradiol was then added to the liquid culture to induce preexisting COG1 to enter the nucleus. The expression of PIF4 and PIF5 was rapidly activated following estradiol induction, demonstrating that COG1 can directly regulate the transcription of PIF4 and PIF5 (Fig. 6A). Previous studies demonstrated that Dof-type transcription factors bind to the 5'-A/TAAAG-3' core sequences or their reversibly complementary sequences 5'-CTTTA/T-3' in the promoters of their target genes to regulate gene expression in Arabidopsis (*Arabidopsis thaliana*; Yanagisawa, 2004). Sequence scanning revealed that there are several putative Dof DNA-binding motifs in the promoter regions of PIF4 and PIF5 (Fig. 6B). To determine whether COG1 associates with these motifs in the PIF4 and PIF5 promoters, 35S:FLAG-COG1 transgenic plants were used for ChIP assays. After immunoprecipitation of protein-DNA complexes from 7-d-old seedlings using an antibody against the FLAG epitope, enriched DNA fragments were amplified by qRT-PCR using primers that annealed near the Dof-binding motifs in the promoters of PIF4 and PIF5. Our results showed that at least one fragment in the PIF4 or PIF5 promoter region was indeed enriched in the ChIP assays, suggesting that COG1 associates directly with the promoters of PIF4 and PIF5 (Fig. 6C).

To further confirm the direct binding of COG1 to the PIF4 and PIF5 promoters, we performed an electrophoretic mobility shift assay (EMSA) using purified GST-COG1 fusion protein from *Escherichia coli*. Our

**Figure 5.** PIF4 and PIF5 are essential for COG1 to promote BR biosynthesis and hypocotyl elongation. A, Expression levels of *PIF4* and *PIF5* in WS2, *cog1-3D*, and *35S:FLAG-COG1* seedlings. One-week-old WS2, *cog1-3D*, and *35S:FLAG-COG1* seedlings were harvested for RNA extraction and qRT-PCR analyses. B, Expression levels of *PIF4* and *PIF5* in WS2 and *GVG:COG1-SRDX* transgenic plants with or without DEX treatment. WS2 and *GVG:COG1-SRDX* seedlings were treated with either mock solution (DMSO) or 10  $\mu$ M DEX for 24 h before harvesting for RNA extraction and qRT-PCR analyses. C and D, Phenotypes and hypocotyl measurements of WS2, *cog1-3D*, *pif4*, *pif4 cog1-3D*, *pif5*, *pif5 cog1-3D*, *pif4 pif5*, and *pif4 pif5 cog1-3D* seedlings. The *pif4 pif5* double mutant was crossed with *cog1-3D* to yield a *pif4 pif5 cog1-3D* triple mutant that was then backcrossed with WS2 for at least five generations. E, qRT-PCR analysis of *CPD*, *DWF4*, *ROT3*, and *BR6ox2* in WS2, *pif4 pif5*, and *pif4 pif5 cog1-3D* seedlings.



results showed that GST-COG1 bound to the biotin-labeled Dof-binding motif-containing DNA fragments in the promoters of *PIF4* and *PIF5*, as suggested by the ChIP assay (Fig. 6D). Furthermore, the binding could be competed off by adding an excessive amount of unlabeled same DNA fragments. However, the unlabeled DNA probes containing mutated Dof-binding motifs failed to compete off the binding of COG1 to the biotin-labeled wild-type DNA fragments (Fig. 6D). Control experiments indicated that GST protein alone failed to bind to the labeled DNA probes (Fig. 6D). Taken together, we conclude that COG1 can bind directly to the promoter region of *PIF4* and *PIF5* and directly enhance their expression.

#### PIF4 and PIF5 Directly Regulate the Expression of *DWF4* and *BR6ox2*

Two pieces of evidence suggest that PIF4 and PIF5 might directly regulate the expression of BR biosynthetic genes. First, COG1 regulation of the expression of BR biosynthetic genes is dependent on PIF4 and PIF5 (Fig. 5E). Second, the transcript levels of *BR6ox2* are reduced significantly in *pif4 pif5* double mutants compared with those in the wild type (Fig. 5E). Given the fact that PIFs bind to the G-box motifs in their target gene promoters, we searched for G-box motifs in the promoters of *CPD*, *DWF4*, *ROT3*, and *BR6ox2*. G-box motifs were found in the promoters of *CPD*, *DWF4*, and

*BR6ox2* but not in the promoter of *ROT3* (Fig. 7A; Supplemental Fig. S12A). To test whether PIF4 and PIF5 bind to the G-box-containing regions of these three BR biosynthetic genes, we performed ChIP assays using the *35S:PIF4-FLAG* and *35S:PIF5-FLAG* transgenic plants and anti-FLAG antibody. PCR analyses indicated that PIF4-FLAG specifically associates with the G-box-containing promoter regions of *CPD*, *DWF4*, and *BR6ox2* (Fig. 7B; Supplemental Fig. S12B). PIF5-FLAG associates with the G-box-containing promoter region of *DWF4* but not with the promoter regions of *CPD* and *BR6ox2* (Fig. 7B). EMSA experiments using PIF4 and PIF5 proteins expressed *in vitro* further confirmed that PIF4 directly bound to the G-box-containing DNA fragments in the promoter regions of *DWF4* and *BR6ox2* (Fig. 7, C and D). PIF5 specifically bound to the G-box-containing DNA fragments in the promoter region of *DWF4* (Fig. 7E). The binding could be effectively competed off by the addition of an excessive amount of unlabeled G-box-containing DNA probes (Fig. 7, C–E). As a control, DNA probes containing a mutated G-box motif (CACGGG) failed to compete off the binding of PIF4 or PIF5 to the biotin-labeled DNA fragments (Fig. 7, C–E). Moreover, we examined whether PIF4 and PIF5 regulate the expression of *DWF4* and *BR6ox2* in planta. qRT-PCR analysis showed that the expression of *DWF4* and *BR6ox2* is significantly up-regulated in both *35S:PIF4* and *35S:PIF5* transgenic plants relative to wild-type seedlings (Fig. 7F). PIF4 was taken as an example to further confirm that this regulation is via a

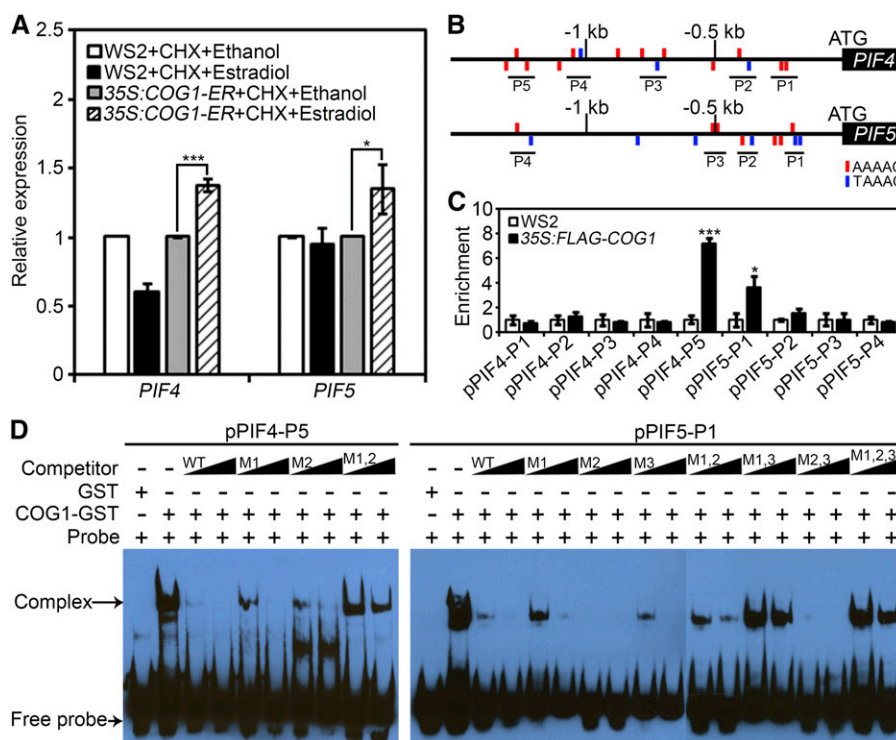


**Figure 6.** COG1 interacts directly with the promoters of *PIF4* and *PIF5*. **A**, Expression levels of *PIF4* and *PIF5* in WS2 and 35S: *COG1-ER* transgenic plants with or without estradiol treatment in the presence of CHX. WS2 and 35S: *COG1-ER* seedlings were pretreated with 10  $\mu$ M CHX for 2 h, then either mock solution (ethanol) or 10  $\mu$ M estradiol was added to the liquid solution for another 2 h before harvesting for RNA extraction and qRT-PCR analyses. **B**, *PIF4* and *PIF5* promoter regions contain multiple Dof motifs (red or blue upright lines). P1 to P5 indicate the DNA fragments amplified in ChIP-PCR assays. **C**, ChIP-quantitative PCR assays showing that COG1 associates with the promoters of *PIF4* and *PIF5* in vivo. One-week-old WS2 and 35S: *FLAG-COG1* seedlings were harvested for ChIP experiments. qRT-PCR was used to quantify enriched DNA fragments in the *PIF4* and *PIF5* promoters. **D**, EMSA showing that COG1 binds to the Dof motifs in the promoter regions of *PIF4* and *PIF5* in vitro. The enriched DNA fragments in the promoters of *PIF4* and *PIF5* were incubated with GST-COG1 recombinant proteins as indicated. GST proteins were used as negative controls. Competition for COG1 binding was performed with 100 $\times$  and 200 $\times$  unlabeled probes containing the enriched DNA fragments (wild type [WT]) or mutated DNA fragments (M).

direct process. Consistently, the expression of *DWF4* and *BR6ox2* can be rapidly up-regulated in 35S: *PIF4-ER* transgenic plants upon the treatment with estradiol in the presence of CHX (Fig. 7G). As a result, the final product of the BR biosynthetic pathway, BL, is increased significantly in 35S: *PIF4* and 35S: *PIF5* transgenic plants (Fig. 7H). Together, these results corroborated that PIF4 and PIF5 redundantly and directly regulate the expression of *DWF4* and *BR6ox2* to promote BR biosynthesis and hypocotyl elongation.

## DISCUSSION

Regarding BR related research, the least characterized aspect is probably the mechanisms controlling BR homeostasis. Consistent with other growth-promoting phytohormones, such as auxin, GA, and cytokinin, both deficiency and excessive amounts of BR are harmful to plant growth and development. Unlike other phytohormones, BRs cannot be transported in a long-distance manner. Therefore, controlling BR homeostasis in a

certain tissue or a cell is extremely important to their biological functions. In this study, we identified a dominant genetic suppressor, *cog1-3D*, of a weak BR receptor mutant named *bri1-5*. *cog1-3D* and *cog1-3D bri1-5* showed significantly longer hypocotyl phenotypes relative to their corresponding backgrounds, WS2 and *bri1-5*, respectively (Figs. 1A and 2A). BR profile analyses revealed that multiple BR intermediates, including two biologically active forms, CS and BL, are drastically elevated in *cog1-3D* in comparison with those in wild-type seedlings (Fig. 3C). Transcription assays ruled out the possibility that it was caused by decreasing BR catabolism. Rather, it appeared that the accumulation of BRs is most likely caused by the enhanced BR biosynthesis. Consistently, several key BR biosynthesis genes are up-regulated in *cog1-3D* (Fig. 4A). Detailed analyses further suggested that *cog1-3D* up-regulation of the expression of BR biosynthetic genes is largely dependent on the function of PIF4 and PIF5. In the *pif4 pif5* background, *cog1-3D* cannot promote the expression of BR biosynthetic genes and, as a result, fails to enhance hypocotyl growth (Fig. 5, C–E).



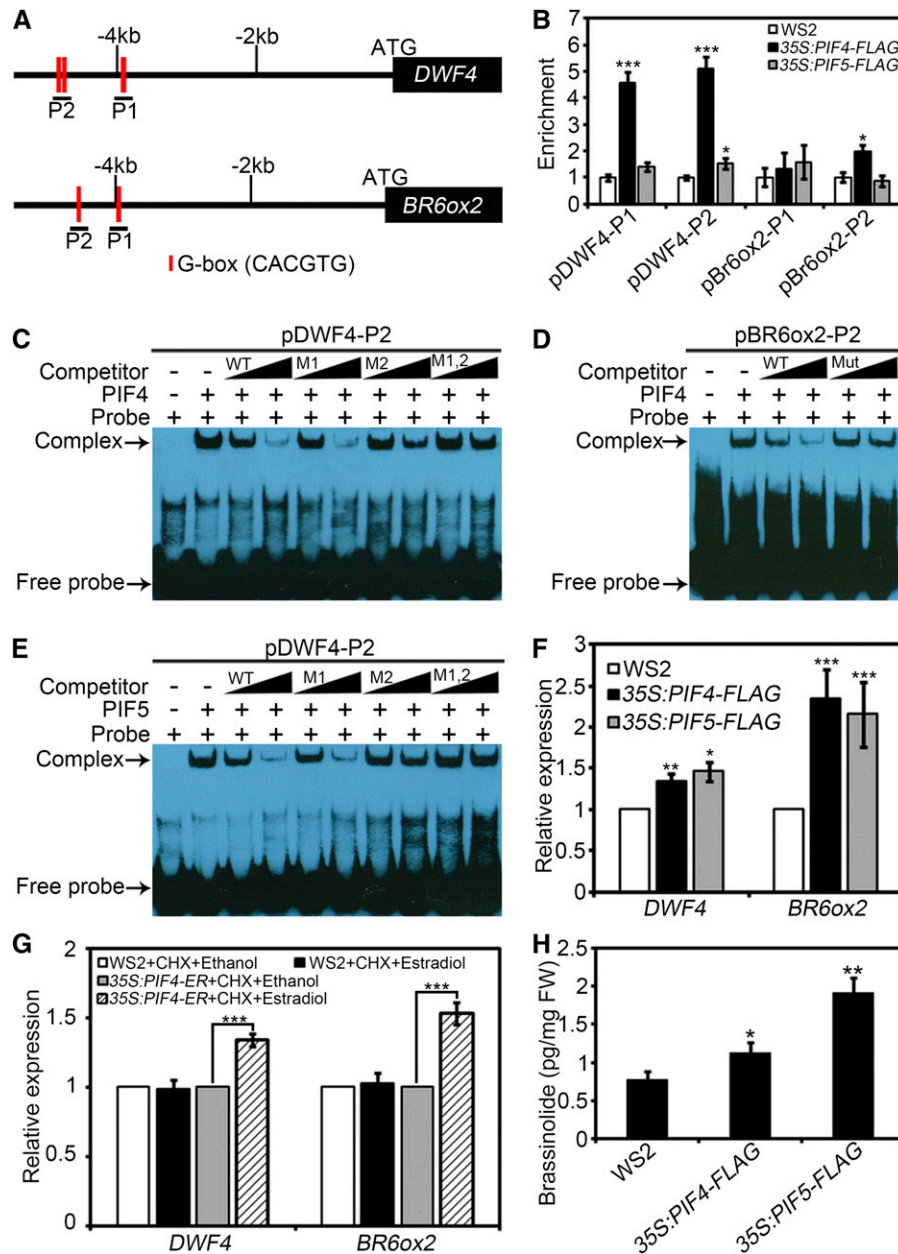


**Figure 7.** PIF4 and PIF5 bind directly to the promoter regions of BR biosynthetic genes and activate their expression. A, Schematic diagrams of the promoter regions of two BR biosynthetic genes, *DWF4* and *BR6ox2*. Red upright lines represent G-box DNA motifs. P1 and P2 are the DNA fragments for ChIP-PCR amplification. B, ChIP analysis showing that PIF4-FLAG and PIF5-FLAG interact with the G-box-containing regions within the *DWF4* and *BR6ox2* promoters upon precipitation with anti-FLAG antibody. One-week-old WS2, *35S:PIF4-FLAG*, and *35S:PIF5-FLAG* seedlings were harvested for ChIP experiments. qRT-PCR was used to quantify the enriched DNA fragments in the *DWF4* and *BR6ox2* promoters. C and D, EMSA indicates that PIF4 binds to the G-box motifs within the promoter regions of *DWF4* and *BR6ox2*. The biotin-labeled probes containing the G-box elements were incubated with TNT-expressed PIF4 protein, which was used for gel-shift analyses. The probes incubated with the TNT expression system without the PIF4 template were used as negative controls. Nonlabeled probes containing G-box (wild type [WT]) or mutated G-box (M) with 10- or 100-fold molar concentrations over the biotin-labeled probe were used as cold competitors. E, EMSA shows that PIF5 binds to the G-box motifs in the promoter of *DWF4*. The fragments containing the G-box motifs present in the promoters of *DWF4* were incubated with TNT-expressed PIF5 protein, which was used subsequently for EMSA analyses. Competition for PIF5 binding was performed using 10- and 100-fold unlabeled probes containing G-box or mutated G-box. F, *DWF4* and *BR6ox2* expression levels in 1-week-old WS2, *35S:PIF4-FLAG*, and *35S:PIF5-FLAG* seedlings. G, Expression levels of *DWF4* and *BR6ox2* in WS2 and *35S:PIF4-ER* transgenic plants with or without estradiol treatment in the presence of CHX. WS2 and *35S:PIF4-ER* seedlings were pretreated with 10  $\mu$ M CHX for 2 h, then either mock solution (ethanol) or 10  $\mu$ M estradiol was added to the liquid solution for another 2 h before harvesting for RNA extraction and qRT-PCR analyses. H, Endogenous BL levels in WS2, *35S:PIF4-FLAG*, and *35S:PIF5-FLAG* seedlings. The data shown are averages and SD from three independent replicates. FW, Fresh weight.

EMSA experiments clearly indicated that COG1 binds directly to the promoter regions of *PIF4* and *PIF5* to regulate their expression. PIF4 and PIF5 associate with G-box motifs in the promoters of *DWF4* and *BR6ox2* (Figs. 6 and 7). Our results obtained from genetic, physiological, and biochemical analyses provide strong evidence to support that COG1 modulates BR biosynthesis and hypocotyl growth via PIF4 and PIF5 in Arabidopsis.

How can we explain the role of COG1 in promoting hypocotyl elongation in the wild type or a weak allele of the *BRI1* mutant but not in BR-deficient mutants or a *BRI1* null mutant? Our current observations suggest that COG1 activates the expression of *PIF4* and *PIF5*, which subsequently enhance BR biosynthesis and signal transduction to promote hypocotyl growth. In the wild-type background, *BRI1*- and *BAK1*-mediated BR signaling results in the dephosphorylation and activation of a BZR1-PIF4 transcription factor complex that regulates the expression of a large number of genes involved in cell elongation to modulate hypocotyl growth (Wang et al., 2002b; Oh et al., 2012; Bernardo-García et al., 2014). COG1 up-regulates the expression of *PIF4* and *PIF5*, enhancing the function of the BZR1-PIF4 complex on hypocotyl elongation. In addition, PIF4 and PIF5 also promote BR biosynthesis, leading to elevated BR signaling, thus further enhancing the function of the BZR1-PIF4 complex (Fig. 8A). In the *bri1-5* background, however, BR signaling is partially impaired. Since BRs are largely accumulated in *bri1-5* (Noguchi et al., 1999a), the elevation of BR biosynthesis alone cannot explain the hypocotyl growth seen in *cog1-3D bri1-5*. It is likely that the elevated PIF4 promotes the complex formation with a leaky amount of nucleus-localized functional BZR1 to regulate downstream

gene expression and slightly enhance hypocotyl growth in *bri1-5* (Fig. 8B). In BR signaling or biosynthesis null mutants, BZR1 and PIF4 are phosphorylated by BIN2, leading to their degradation (He et al., 2002; Bernardo-García et al., 2014). Thus, COG1-mediated up-regulation of PIF4 cannot promote the formation of the BZR1-PIF4 complex and fails to enhance hypocotyl growth (Fig. 8C). These results indicated that the function of COG1 in regulating hypocotyl growth is dependent on both PIF4 and BRs.

PIF4 and PIF5 were found initially to interact directly with PHYB and act as its downstream components to mediate phytochrome signaling (Huq and Quail, 2002; Shen et al., 2007). Recent studies suggested that they are the main integrators in light and hormonal signaling pathways to mediate hypocotyl elongation (de Lucas et al., 2008; Bai et al., 2012; Gallego-Bartolomé et al., 2012; Oh et al., 2012, 2014; Bernardo-García et al., 2014). PIF4 interacts directly with BZR1 and ARF6 to coregulate a large number of target genes critical for cell expansion, providing evidence for the cross talk among BR, auxin, and phytochrome during hypocotyl growth (Oh et al., 2014). Furthermore, GA promotes cell elongation largely by releasing the DELLA-mediated repression of PIF4, BZR1, and ARF6 (Bai et al., 2012; Gallego-Bartolomé et al., 2012). In addition to DELLA proteins, the activity and levels of PIF4 are regulated by several other mechanisms. Interaction with the Pfr form of PHYB induces the phosphorylation and degradation of PIF4 (Huq and Quail, 2002; Shen et al., 2007). A recent study found that BIN2 phosphorylates PIF4 to bring it to a degradation pathway (Bernardo-García et al., 2014). Additionally, the expression of *PIF4* can be induced in response to far-red and red light (Huq and Quail, 2002). Temperature and the circadian clock also

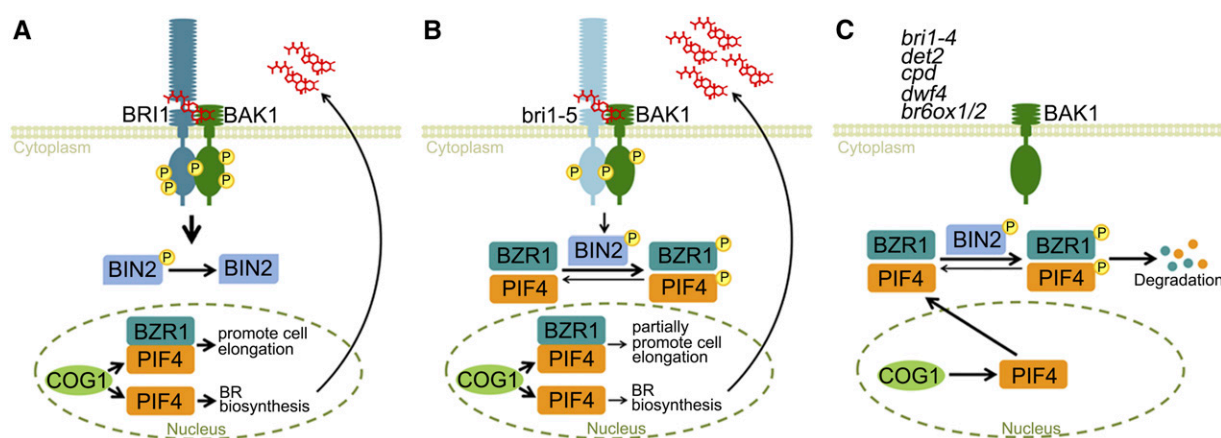


**Figure 8.** A model for COG1 promoting hypocotyl elongation. A, In the wild-type background, COG1 activates the expression of *PIF4*, which not only enhances the function of the BZR1-PIF4 complex on hypocotyl elongation but also promotes BR biosynthesis, further enhancing BR signaling and, thus, the function of BZR1-PIF4 on cell elongation. B, In the *bri1-5* background, the elevation of BR biosynthesis has no effect on hypocotyl growth, since BR signaling is partially impaired. However, the elevated PIF4 by COG1 promotes the complex formation of BZR1-PIF4 and, thus, downstream gene expression to partially enhance hypocotyl growth in *bri1-5*. C, In BR signaling or biosynthesis null mutants, BZR1 and PIF4 are phosphorylated by BIN2, leading to their degradation. Thus, the COG1-mediated up-regulation of *PIF4* fails to enhance hypocotyl growth.

control the transcription levels of *PIFs* (Leivar and Quail, 2011). However, the transcription factors that directly regulate the expression of *PIF4* are largely unknown. A previous study revealed that *COG1* expression could be induced by far-red and red light, which is similar to that of *PIF4* (Huq and Quail, 2002; Park et al., 2003). In this study, we demonstrated that *COG1* binds directly to the promoter regions of *PIF4* and *PIF5* to regulate their expression (Fig. 6).

Biosynthetic pathways are frequently feedback regulated by their end products or their signaling pathway either positively or negatively. For example, ethylene can both positively and negatively regulate its biosynthesis by up-regulating the expression of *ACS2* and *ACS4* and down-regulating the expression of *ACS6* (Wang et al., 2002a). Abscisic acid induces the expression of *AtNCED3* to positively regulate its biosynthesis under dehydration stress (Yang and Tan, 2014). BR signaling is utilized to create a feedback inhibitory regulation loop to control the expression of BR biosynthetic genes (He et al., 2005; Sun et al., 2010; Yu et al., 2011). Together with previous studies, our results support a positive feedback regulatory loop of BR biosynthesis by *PIF4*-mediated signaling (Fig. 8). In the absence of BR, *BIN2* phosphorylates *PIF4*, leading to its degradation process and the inhibition of hypocotyl elongation (Bernardo-García et al., 2014). In the presence of BR, activated *BRI1* and *BAK1* receptor kinase lead to the inactivation of *BIN2*. *PIF4* then can interact with *BZR1* to regulate the expression of their target genes and promote hypocotyl growth (Oh et al., 2012; Bernardo-García et al., 2014). On the other hand, *PIF4* activates the expression of *DWF4* and *BR6ox2* to produce more BRs and further promote hypocotyl elongation. Meanwhile, *BZR1* can inhibit the expression of BR biosynthetic genes when BRs are excessive to plant growth and development (He et al., 2005). Such positive and negative feedback loops ensure optimal BR effects on plant growth and development. How plants reset the equilibrium of BR in response to developmental and environmental signals is a question to be answered in the near future.

Understanding the mechanisms controlling BR homeostasis can help us to develop strategies to optimize plant growth and development via genetic engineering in the future. BR profile analysis showed that the substrates of *DWF4* are always plentiful in plants. However, the products of the *DWF4*-catalyzed reactions are considerably low or even undetectable, suggesting that *DWF4* catalyzes a flux-determining step in BR biosynthesis (Guo et al., 2010). *BR6ox2* was identified as a bifunctional enzyme that mediates the conversion of CS to BL, the final and rate-limiting step in BR biosynthesis, as well as BR C-6 oxidation (Kim et al., 2005). Controlling the expression of *DWF4* and/or *BR6ox2* could be an effective approach to alter BR production in response to external and internal cues. *TCP1* was identified as a transcription factor promoting the expression of *DWF4* (Guo et al., 2010). Auxin and high temperature also can induce the expression of *DWF4*

via mechanisms yet to be determined (Chung et al., 2011; Maharjan and Choe, 2011). However, transcriptional regulation of *BR6ox2* is not described in the literature. Our data revealed that *PIF4* functions as a positive regulator enhancing the expression of *DWF4* and *BR6ox2*, leading to an increase of bioactive levels of BRs in *cog1-3D* (Figs. 3C and 7). *PIF5*, a homolog of *PIF4*, also can bind to the promoter of *DWF4* to activate its expression (Fig. 7).

Interestingly, *CPD* also is up-regulated in *COG1*- and *PIF4*-overexpressing plants, and the ChIP assay showed that *PIF4* associates with the promoter of *CPD* (Fig. 4A; Supplemental Fig. S12C). However, we failed to detect the direct binding of *PIF4* to the *CPD* promoter, indicating the existence of other transcription factors that regulate *CPD* expression together with *PIF4*. The expression levels of *CPD* and *DWF4* are not altered significantly in *pif4 pif5* double mutants compared with the wild type (Fig. 5E), which should be caused by the functional redundancy of other transcription factors, such as *CES* and *TCP1*, that regulate the expression of these two BR biosynthetic genes. And there might be more transcription factors regulating the level of these two BR biosynthetic genes. Teasterone, an earlier BR intermediate converted from cathasterone by *ROT3*, also is increased in *cog1-3D* (Fig. 3C). However, *ROT3* is not regulated directly by *PIF4* and *PIF5*, suggesting that *COG1* may regulate *ROT3* expression through other transcription factors. Typhasterol and CS are both elevated in *cog1-3D*, indicating that *COG1* regulates genes essential for C-3 dehydrogenation, C-3 reduction, and C-2 hydroxylation. It is known that *Osd2* and *Osd11* are responsible for the C-3 dehydrogenation and C-3 reduction reactions in rice (*Oryza sativa*), respectively (Hong et al., 2003; Tanabe et al., 2005). C-2 hydroxylation of BRs is mediated by *DDWF1* in pea (*Pisum sativum*; Kang et al., 2001). However, the enzymes catalyzing these reactions in Arabidopsis are not identified. It is possible that homologs of these three cytochrome P450s that are up-regulated in *cog1-3D* are the potential enzymes responsible for the corresponding reactions in Arabidopsis.

## MATERIALS AND METHODS

### Plant Materials

The Arabidopsis (*Arabidopsis thaliana*) *bri1-5 cog1-3D* double mutant was obtained from a large-scale activation-tagging screen for *bri1-5* genetic modifiers as described previously (Li et al., 2001, 2002; Yuan et al., 2007; Guo et al., 2010). The *cog1-3D* single mutant was generated by backcrossing *bri1-5 cog1-3D* with WS2. Other plant materials, including *bri1-5*, *bri1-4*, *det2*, *cpd*, *dwf4*, and *cog1-D*, were described previously (Noguchi et al., 1999a; Park et al., 2003; Guo et al., 2010). The *cog1-6* mutant was identified from an ethyl methanesulfonate-mutagenized *cog1-D* seed pool. The *br6ox1* (Salk\_148384), *br6ox2* (Salk\_148384), *pif4* (Salk\_140393), and *pif5* (Salk\_087012) T-DNA insertion lines were obtained from the Arabidopsis Biological Resource Center. The *bri1-5*, *bri1-4*, *det2*, and *dwf4* mutants are in the WS2 background. The *cpd*, *br6ox1/2*, *pif4*, and *pif5* mutants are in the Columbia-0 background. The double or triple mutants were generated by genetic crossing using the related single mutants. The *cpd cog1-3D*, *br6ox1/2 cog1-3D*, and *pif4 pif5 cog1-3D* mutants were then backcrossed with the WS2 ecotype for at least five times.

## Identification of the *cog1-3D* Locus

The flanking genomic sequence of the inserted T-DNA of *pBIB-BASTA-AT2* was amplified using thermal asymmetric interlaced PCR as described previously (Liu and Whittier, 1995; Yuan et al., 2007; Guo et al., 2010). The T-DNA insertion site was determined by sequencing the flanking genomic DNA.

## Constructs and Plant Transformation

Gateway technology was employed to clone the coding sequences of *COG1*, *PIF4*, and *PIF5* (Gou et al., 2010). The amplified *COG1* coding sequence was cloned into a *pEarleyGate 202* destination vector (Earley et al., 2006). The *PIF4* and *PIF5* coding sequences were cloned into a *pBIB-35S-GWR-FLAG* vector (Gou et al., 2010). For the construction of *35S:COG1-ER* and *35S:PIF4-ER*, the coding sequences of these two genes were introduced in a *pBIB-35S-GWR-ER* vector. For the construction of *35S:COG1-SRDX* and *GVG:COG1-SRDX*, *COG1-SRDX* was PCR amplified and introduced in a *pBIB-35S-GWR* vector and a Gateway-compatible *pTA7002* vector (Aoyama and Chua, 1997; Gou et al., 2010). These expression constructs were then transformed into *Agrobacterium tumefaciens* strain GV3101 for transformation of Arabidopsis plants by the floral dip method (Clough and Bent, 1998). The primers used are listed in Supplemental Table S2.

## Hypocotyl Measurements

Seeds were surface sterilized for 15 min in 10% bleach, washed five times with sterilized water, and planted on one-half-strength MS agar plates containing 1% (w/v) Suc, with or without 24-epiBL, or BRZ. Plants were pretreated at 4°C for 3 d and then transferred to a growth chamber set at 22°C with a 16-h-light/8-h-dark photoperiod or in continuous red light for 6 d. The *GVG:COG1-SRDX* seeds were planted on one-half-strength MS agar plates containing 1% (w/v) Suc. Two days after germination, the seedlings were transferred to one-half-strength MS agar plates containing 1% (w/v) Suc and 10 μM DEX, growing for another 5 d. Hypocotyls of the seedlings were then scanned and measured as reported previously (Yuan et al., 2007). All measurements were repeated three times, and at least 20 seedlings were measured for each genotype. Student's *t* test was performed (\*, *P* < 0.05; \*\*, *P* < 0.01; and \*\*\*, *P* < 0.001).

## qRT-PCR Analyses

Long-day-grown seedlings were harvested directly or after treatment with DEX or estradiol and CHX at the same time of day and frozen in liquid nitrogen for RNA extraction. Total RNA was extracted using the RNeasy Pure Plant Kit (Qiagen). Five micrograms of total RNA was reverse transcribed into first-strand cDNAs using M-MLV reverse transcriptase (Thermo Fisher Scientific) according to the manufacturer's instructions. The cDNA samples diluted 10-fold were used as PCR templates. qRT-PCR was performed using SYBR Premix Ex Taq II (TaKaRa) on a Step One Plus Real-Time PCR machine (Thermo Fisher Scientific). The relative expression level was calculated from three replicates using the  $\Delta\Delta C_t$  method after normalization to an *ACT2* control. All the qRT-PCR analyses were performed for three biological replicates, yielding similar results. Data shown are means and SE from three biological replicates. Student's *t* test was performed (\*, *P* < 0.05; \*\*, *P* < 0.01; \*\*\*, *P* < 0.001; and ns, not significant). The primers used are listed in Supplemental Table S2.

## BR Profile Assays

Samples were analyzed for BR contents as described previously with a few modifications (Swaczynova et al., 2007). Briefly, 50 mg of fresh Arabidopsis tissue samples was homogenized to a fine consistency using 3-mm zirconium oxide beads and an MM 301 vibration mill at a frequency of 30 Hz for 3 min (Retsch). The samples were then extracted overnight with stirring at 4°C using a benchtop laboratory rotator (Stuart SB3; Bibby Scientific) after the addition of 1 mL of ice-cold 60% acetonitrile and 10 pmol of [<sup>2</sup>H<sub>3</sub>]BL, [<sup>2</sup>H<sub>3</sub>]CS, [<sup>2</sup>H<sub>3</sub>]24-epiBL, [<sup>2</sup>H<sub>3</sub>]24-epicastasterone, [<sup>2</sup>H<sub>3</sub>]28-norbrassinolide, and [<sup>2</sup>H<sub>3</sub>]28-norcastasterone as internal standards (OChemIm). The samples were further centrifuged, purified on polyamide SPE columns (Supelco), and then analyzed by ultra-high-performance liquid chromatography-tandem mass spectrometry (Micromass). The data were analyzed using Masslynx 4.1 software (Waters), and BR content was finally quantified by the standard isotope dilution method (Rittenberg and Foster, 1940).

## ChIP-PCR Assay

Two grams of one-week-old WS2, *35S:FLAG-COG1*, *35S:PIF4-FLAG*, and *35S:PIF5-FLAG* transgenic seedlings was harvested for ChIP experiments. Chromatin was isolated and sonicated to generate DNA fragments with an average size of 500 bp. The solubilized chromatin was immunoprecipitated by an agarose-conjugated anti-FLAG antibody (Sigma-Aldrich). The coimmunoprecipitated DNA was recovered and analyzed by quantitative PCR with SYBR Premix Ex Taq II (TaKaRa). Relative fold enrichment was calculated by normalizing the amount of a target DNA fragment against that of an *ACT2* promoter fragment and then against the respective input DNA samples. Three independent biological repeats were performed, yielding similar results. Shown are representative data from one biological replicate. Student's *t* test was performed (\*, *P* < 0.05; \*\*, *P* < 0.01; and \*\*\*, *P* < 0.001). The primers used are listed in Supplemental Table S2.

## DNA Gel-Shift Assay

The full-length *COG1* coding region was cloned into a *pGEX-4T-3* vector (GE). The resulting constructs were sequenced to confirm the correct open reading frame and sequences and then transformed into the *Escherichia coli* Rosetta strain for recombinant protein expression. Bacteria were grown in 100 mL of Luria-Bertani medium supplemented with 100 μg mL<sup>-1</sup> ampicillin and 30 μg mL<sup>-1</sup> chloramphenicol, and the GST-COG1 recombinant proteins were purified with GST-Sefinose Resin (Sangon Biotech). PIF4 and PIF5 were synthesized using the TNT SP6 High-Yield Wheat Germ Protein Expression System (Promega). The probes were synthesized and labeled with biotin using the Biotin 3' End DNA Labeling Kit (Thermo Fisher Scientific). Unlabeled competitor probes were generated from dimerized oligonucleotides. EMSA experiments were performed using the Chemiluminescent Nucleic Acid Detection Module (Thermo Fisher Scientific) according to the manufacturer's instructions. Probe sequences are shown in Supplemental Table S2.

## Accession Numbers

Sequence data from this article can be found in the Arabidopsis Genome Initiative or GenBank/EMBL databases under the following accession numbers: *COG1* (At1g29160), *PIF4* (At2g43010), *PIF5* (At3g59060), *DET2* (At2g38050), *CPD* (At5g05690), *DWF4* (At3g50660), *BR6ox1* (At5g38970), *BR6ox2* (At3g30180), *ROT3* (At4g36380), and *CYP90D1* (At3g13730).

## Supplemental Data

The following supplemental materials are available.

**Supplemental Figure S1.** The *cog1-6* mutant was identified as an intragenic suppressor of *cog1-D*.

**Supplemental Figure S2.** Phenotypes of *35S:COG1-SRDX* transgenic plants.

**Supplemental Figure S3.** Induced expression of *COG1-SRDX* leads to reduced cell length.

**Supplemental Figure S4.** BR signal transduction is elevated in the *cog1-3D* mutant.

**Supplemental Figure S5.** BRZ inhibits the hypocotyl growth of *cog1-3D* seedlings.

**Supplemental Figure S6.** Expression of *DET2*, *CYP90D1*, and *BR6ox1* in *cog1-3D*.

**Supplemental Figure S7.** Expression of BR catabolism genes in *cog1-3D*.

**Supplemental Figure S8.** The *bri1-4* mutation completely inhibits the long-hypocotyl phenotype of *cog1-3D*.

**Supplemental Figure S9.** PIF4 and PIF5 promote cell elongation.

**Supplemental Figure S10.** Protein levels of PIF5 in *cog1-3D* and *35S:FLAG-COG1* seedlings.

**Supplemental Figure S11.** *COG1*-mediated hypocotyl elongation is dependent on PIF4 and PIF5.

**Supplemental Figure S12.** PIF4 regulates the expression of *CPD*.

**Supplemental Table S1.** The expression of 37 transcription factors is significantly altered in *cog1-3D* compared with WS2.

**Supplemental Table S2.** List of primers and probes used in this study.

## ACKNOWLEDGMENTS

We thank Dr. Yanhai Yin (Iowa State University) and Dr. Haodong Chen (Peking University) for providing the BES1 and PIF5 antibodies, respectively.

Received November 21, 2016; accepted April 21, 2017; published April 24, 2017.

## LITERATURE CITED

- Aoyama T, Chua NH (1997) A glucocorticoid-mediated transcriptional induction system in transgenic plants. *Plant J* **11**: 605–612
- Asami T, Min YK, Nagata N, Yamagishi K, Takatsuto S, Fujioka S, Murofushi N, Yamaguchi I, Yoshida S (2000) Characterization of brassinazole, a triazole-type brassinosteroid biosynthesis inhibitor. *Plant Physiol* **123**: 93–100
- Bai MY, Shang JX, Oh E, Fan M, Bai Y, Zentella R, Sun TP, Wang ZY (2012) Brassinosteroid, gibberellin and phytochrome impinge on a common transcription module in Arabidopsis. *Nat Cell Biol* **14**: 810–817
- Bajguz A (2007) Metabolism of brassinosteroids in plants. *Plant Physiol Biochem* **45**: 95–107
- Bancoş S, Nomura T, Sato T, Molnár G, Bishop GJ, Koncz C, Yokota T, Nagy F, Szekeres M (2002) Regulation of transcript levels of the Arabidopsis cytochrome p450 genes involved in brassinosteroid biosynthesis. *Plant Physiol* **130**: 504–513
- Bernardo-García S, de Lucas M, Martínez C, Espinosa-Ruiz A, Davière JM, Prat S (2014) BR-dependent phosphorylation modulates PIF4 transcriptional activity and shapes diurnal hypocotyl growth. *Genes Dev* **28**: 1681–1694
- Bishop GJ, Nomura T, Yokota T, Harrison K, Noguchi T, Fujioka S, Takatsuto S, Jones JD, Kamiya Y (1999) The tomato DWARF enzyme catalyses C-6 oxidation in brassinosteroid biosynthesis. *Proc Natl Acad Sci USA* **96**: 1761–1766
- Bueso E, Muñoz-Bertomeu J, Campos F, Martínez C, Tello C, Martínez-Almonacid I, Ballester P, Simón-Moya M, Brunaud V, Yenush L, et al (2016) Arabidopsis COGWHEEL1 links light perception and gibberellins with seed tolerance to deterioration. *Plant J* **87**: 583–596
- Castillon A, Shen H, Huq E (2007) Phytochrome Interacting Factors: central players in phytochrome-mediated light signaling networks. *Trends Plant Sci* **12**: 514–521
- Choe S, Dilkes BP, Fujioka S, Takatsuto S, Sakurai A, Feldmann KA (1998) The *DWF4* gene of Arabidopsis encodes a cytochrome P450 that mediates multiple 22 $\alpha$ -hydroxylation steps in brassinosteroid biosynthesis. *Plant Cell* **10**: 231–243
- Choi YH, Fujioka S, Harada A, Yokota T, Takatsuto S, Sakurai A (1996) A brassinolide biosynthetic pathway via 6-deoxocastasterone. *Phytochemistry* **43**: 593–596
- Choi YH, Fujioka S, Nomura T, Harada A, Yokota T, Takatsuto S, Sakurai A (1997) An alternative brassinolide biosynthetic pathway via late C-6 oxidation. *Phytochemistry* **44**: 609–613
- Chory J, Nagpal P, Peto CA (1991) Phenotypic and genetic analysis of *det2*, a new mutant that affects light-regulated seedling development in Arabidopsis. *Plant Cell* **3**: 445–459
- Chung Y, Maharjan PM, Lee O, Fujioka S, Jang S, Kim B, Takatsuto S, Tsujimoto M, Kim H, Cho S, et al (2011) Auxin stimulates *DWARF4* expression and brassinosteroid biosynthesis in Arabidopsis. *Plant J* **66**: 624–638
- Clough SJ, Bent AF (1998) Floral dip: a simplified method for Agrobacterium-mediated transformation of Arabidopsis thaliana. *Plant J* **16**: 735–743
- Clouse SD, Sasse JM (1998) Brassinosteroids: essential regulators of plant growth and development. *Annu Rev Plant Physiol Plant Mol Biol* **49**: 427–451
- de Lucas M, Davière JM, Rodríguez-Falcón M, Pontin M, Iglesias-Pedraz JM, Lorrain S, Fankhauser C, Blázquez MA, Titarenko E, Prat S (2008) A molecular framework for light and gibberellin control of cell elongation. *Nature* **451**: 480–484
- Earley KW, Haag JR, Pontes O, Opper K, Juehne T, Song K, Pikaard CS (2006) Gateway-compatible vectors for plant functional genomics and proteomics. *Plant J* **45**: 616–629
- Fujioka S, Inoue T, Takatsuto S, Yanagisawa T, Yokota T, Sakurai A (1995) Identification of a new brassinosteroid, cathasterone, in cultured-cells of catharanthus-roseus as a biosynthetic precursor of teasterone. *Biosci Biotechnol Biochem* **59**: 1543–1547
- Fujioka S, Li J, Choi YH, Seto H, Takatsuto S, Noguchi T, Watanabe T, Kuriyama H, Yokota T, Chory J, et al (1997) The Arabidopsis *deetiolated2* mutant is blocked early in brassinosteroid biosynthesis. *Plant Cell* **9**: 1951–1962
- Fujioka S, Takatsuto S, Yoshida S (2002) An early C-22 oxidation branch in the brassinosteroid biosynthetic pathway. *Plant Physiol* **130**: 930–939
- Fujioka S, Yokota T (2003) Biosynthesis and metabolism of brassinosteroids. *Annu Rev Plant Biol* **54**: 137–164
- Fujita S, Ohnishi T, Watanabe B, Yokota T, Takatsuto S, Fujioka S, Yoshida S, Sakata K, Mizutani M (2006) Arabidopsis CYP90B1 catalyses the early C-22 hydroxylation of C27, C28 and C29 sterols. *Plant J* **45**: 765–774
- Gallego-Bartolomé J, Minguet EG, Grau-Enguix F, Abbas M, Locascio A, Thomas SG, Alabadi D, Blázquez MA (2012) Molecular mechanism for the interaction between gibberellin and brassinosteroid signaling pathways in Arabidopsis. *Proc Natl Acad Sci USA* **109**: 13446–13451
- Gao Y, Zhang D, Li J (2015) TCP1 modulates *DWF4* expression via directly interacting with the GGNCCC motifs in the promoter region of *DWF4* in Arabidopsis thaliana. *J Genet Genomics* **42**: 383–392
- Gou X, He K, Yang H, Yuan T, Lin H, Clouse SD, Li J (2010) Genome-wide cloning and sequence analysis of leucine-rich repeat receptor-like protein kinase genes in Arabidopsis thaliana. *BMC Genomics* **11**: 19
- Gou X, Li J (2012) Activation tagging. *Methods Mol Biol* **876**: 117–133
- Gou X, Yin H, He K, Du J, Yi J, Xu S, Lin H, Clouse SD, Li J (2012) Genetic evidence for an indispensable role of somatic embryogenesis receptor kinases in brassinosteroid signaling. *PLoS Genet* **8**: e1002452
- Guo Z, Fujioka S, Blancaflor EB, Miao S, Gou X, Li J (2010) TCP1 modulates brassinosteroid biosynthesis by regulating the expression of the key biosynthetic gene *DWARF4* in Arabidopsis thaliana. *Plant Cell* **22**: 1161–1173
- He JX, Gendron JM, Sun Y, Gampala SS, Gendron N, Sun CQ, Wang ZY (2005) BZR1 is a transcriptional repressor with dual roles in brassinosteroid homeostasis and growth responses. *Science* **307**: 1634–1638
- He JX, Gendron JM, Yang Y, Li J, Wang ZY (2002) The GSK3-like kinase BIN2 phosphorylates and destabilizes BZR1, a positive regulator of the brassinosteroid signaling pathway in Arabidopsis. *Proc Natl Acad Sci USA* **99**: 10185–10190
- He K, Xu S, Li J (2013) BAK1 directly regulates brassinosteroid perception and BRI1 activation. *J Integr Plant Biol* **55**: 1264–1270
- Hiratsu K, Matsui K, Koyama T, Ohme-Takagi M (2003) Dominant repression of target genes by chimeric repressors that include the EAR motif, a repression domain, in Arabidopsis. *Plant J* **34**: 733–739
- Hong Z, Ueguchi-Tanaka M, Umemura K, Uozu S, Fujioka S, Takatsuto S, Yoshida S, Ashikari M, Kitano H, Matsuoka M (2003) A rice brassinosteroid-deficient mutant, *ebisu dwarf (d2)*, is caused by a loss of function of a new member of cytochrome P450. *Plant Cell* **15**: 2900–2910
- Hothorn M, Belkhadir Y, Dreux M, Dabi T, Noel JP, Wilson IA, Chory J (2011) Structural basis of steroid hormone perception by the receptor kinase BRI1. *Nature* **474**: 467–471
- Huq E, Quail PH (2002) PIF4, a phytochrome-interacting bHLH factor, functions as a negative regulator of phytochrome B signaling in Arabidopsis. *EMBO J* **21**: 2441–2450
- Jaillais Y, Hothorn M, Belkhadir Y, Dabi T, Nimchuk ZL, Meyerowitz EM, Chory J (2011) Tyrosine phosphorylation controls brassinosteroid receptor activation by triggering membrane release of its kinase inhibitor. *Genes Dev* **25**: 232–237
- Kang JG, Yun J, Kim DH, Chung KS, Fujioka S, Kim JI, Dae HW, Yoshida S, Takatsuto S, Song PS, et al (2001) Light and brassinosteroid signals are integrated via a dark-induced small G protein in etiolated seedling growth. *Cell* **105**: 625–636
- Kim TW, Guan S, Burlingame AL, Wang ZY (2011) The CDG1 kinase mediates brassinosteroid signal transduction from BRI1 receptor kinase to BSU1 phosphatase and GSK3-like kinase BIN2. *Mol Cell* **43**: 561–571
- Kim TW, Guan S, Sun Y, Deng Z, Tang W, Shang JX, Sun Y, Burlingame AL, Wang ZY (2009) Brassinosteroid signal transduction from cell-surface receptor kinases to nuclear transcription factors. *Nat Cell Biol* **11**: 1254–1260
- Kim TW, Hwang JY, Kim YS, Joo SH, Chang SC, Lee JS, Takatsuto S, Kim SK (2005) Arabidopsis CYP85A2, a cytochrome P450, mediates the

- Baeyer-Villiger oxidation of castasterone to brassinolide in brassinosteroid biosynthesis. *Plant Cell* **17**: 2397–2412
- Kinoshita T, Caño-Delgado A, Seto H, Hiranuma S, Fujioka S, Yoshida S, Chory J** (2005) Binding of brassinosteroids to the extracellular domain of plant receptor kinase BRI1. *Nature* **433**: 167–171
- Leivar P, Quail PH** (2011) PIFs: pivotal components in a cellular signaling hub. *Trends Plant Sci* **16**: 19–28
- Li J, Lease KA, Tax FE, Walker JC** (2001) BRS1, a serine carboxypeptidase, regulates BRI1 signaling in *Arabidopsis thaliana*. *Proc Natl Acad Sci USA* **98**: 5916–5921
- Li J, Nagpal P, Vitart V, McMorris TC, Chory J** (1996) A role for brassinosteroids in light-dependent development of *Arabidopsis*. *Science* **272**: 398–401
- Li J, Nam KH** (2002) Regulation of brassinosteroid signaling by a GSK3/SHAGGY-like kinase. *Science* **295**: 1299–1301
- Li J, Wen J, Lease KA, Doke JT, Tax FE, Walker JC** (2002) BAK1, an *Arabidopsis* LRR receptor-like protein kinase, interacts with BRI1 and modulates brassinosteroid signaling. *Cell* **110**: 213–222
- Liu YG, Whittier RF** (1995) Thermal asymmetric interlaced PCR: automatable amplification and sequencing of insert end fragments from P1 and YAC clones for chromosome walking. *Genomics* **25**: 674–681
- Maharjan PM, Choe S** (2011) High temperature stimulates *DWARF4* (*DWF4*) expression to increase hypocotyl elongation in *Arabidopsis*. *J Plant Biol* **54**: 425–429
- Mathur J, Molnár G, Fujioka S, Takatsuto S, Sakurai A, Yokota T, Adam G, Voigt B, Nagy F, Maas C, et al** (1998) Transcription of the *Arabidopsis* *CPD* gene, encoding a steroidogenic cytochrome P450, is negatively controlled by brassinosteroids. *Plant J* **14**: 593–602
- Mora-García S, Vert G, Yin Y, Caño-Delgado A, Cheong H, Chory J** (2004) Nuclear protein phosphatases with Kelch-repeat domains modulate the response to brassinosteroids in *Arabidopsis*. *Genes Dev* **18**: 448–460
- Nam KH, Li J** (2002) BRI1/BAK1, a receptor kinase pair mediating brassinosteroid signaling. *Cell* **110**: 203–212
- Noguchi T, Fujioka S, Choe S, Takatsuto S, Yoshida S, Yuan H, Feldmann KA, Tax FE** (1999a) Brassinosteroid-insensitive dwarf mutants of *Arabidopsis* accumulate brassinosteroids. *Plant Physiol* **121**: 743–752
- Noguchi T, Fujioka S, Takatsuto S, Sakurai A, Yoshida S, Li J, Chory J** (1999b) *Arabidopsis det2* is defective in the conversion of (24R)-24-methylcholest-4-En-3-one to (24R)-24-methyl-5 $\alpha$ -cholestan-3-one in brassinosteroid biosynthesis. *Plant Physiol* **120**: 833–840
- Oh E, Zhu JY, Bai MY, Arenhart RA, Sun Y, Wang ZY** (2014) Cell elongation is regulated through a central circuit of interacting transcription factors in the *Arabidopsis* hypocotyl. *eLife* **3**: doi/10.7554/eLife.03031
- Oh E, Zhu JY, Wang ZY** (2012) Interaction between BZR1 and PIF4 integrates brassinosteroid and environmental responses. *Nat Cell Biol* **14**: 802–809
- Ohnishi T, Godza B, Watanabe B, Fujioka S, Hategan L, Ide K, Shibata K, Yokota T, Szekeres M, Mizutani M** (2012) CYP90A1/CPD, a brassinosteroid biosynthetic cytochrome P450 of *Arabidopsis*, catalyzes C-3 oxidation. *J Biol Chem* **287**: 31551–31560
- Ohnishi T, Szatmari AM, Watanabe B, Fujita S, Bancos S, Koncz C, Lafos M, Shibata K, Yokota T, Sakata K, et al** (2006) C-23 hydroxylation by *Arabidopsis* CYP90C1 and CYP90D1 reveals a novel shortcut in brassinosteroid biosynthesis. *Plant Cell* **18**: 3275–3288
- Park DH, Lim PO, Kim JS, Cho DS, Hong SH, Nam HG** (2003) The *Arabidopsis* *COG1* gene encodes a Dof domain transcription factor and negatively regulates phytochrome signaling. *Plant J* **34**: 161–171
- Poppenberger B, Rozhon W, Khan M, Husar S, Adam G, Luschnig C, Fujioka S, Sieberer T** (2011) CESTA, a positive regulator of brassinosteroid biosynthesis. *EMBO J* **30**: 1149–1161
- Rittenberg D, Foster GL** (1940) A new procedure for quantitative analysis by isotope dilution, with application to the determination of amino acids and fatty acids. *J Biol Chem* **133**: 737–744
- Santiago J, Henzler C, Hothorn M** (2013) Molecular mechanism for plant steroid receptor activation by somatic embryogenesis co-receptor kinases. *Science* **341**: 889–892
- She J, Han Z, Kim TW, Wang J, Cheng W, Chang J, Shi S, Wang J, Yang M, Wang ZY, et al** (2011) Structural insight into brassinosteroid perception by BRI1. *Nature* **474**: 472–476
- Shen Y, Khanna R, Carle CM, Quail PH** (2007) Phytochrome induces rapid PIF5 phosphorylation and degradation in response to red-light activation. *Plant Physiol* **145**: 1043–1051
- Shimada Y, Fujioka S, Miyauchi N, Kushiro M, Takatsuto S, Nomura T, Yokota T, Kamiya Y, Bishop GJ, Yoshida S** (2001) Brassinosteroid-6-oxidases from *Arabidopsis* and tomato catalyze multiple C-6 oxidations in brassinosteroid biosynthesis. *Plant Physiol* **126**: 770–779
- Sun Y, Fan XY, Cao DM, Tang W, He K, Zhu JY, He JX, Bai MY, Zhu S, Oh E, et al** (2010) Integration of brassinosteroid signal transduction with the transcription network for plant growth regulation in *Arabidopsis*. *Dev Cell* **19**: 765–777
- Sun Y, Han Z, Tang J, Hu Z, Chai C, Zhou B, Chai J** (2013) Structure reveals that BAK1 as a co-receptor recognizes the BRI1-bound brassinolide. *Cell Res* **23**: 1326–1329
- Suzuki H, Fujioka S, Takatsuto S, Yokota T, Murofushi N, Sakurai A** (1993) Biosynthesis of brassinolide from castasterone in cultured cells of *Catharanthus roseus*. *J Plant Growth Regul* **12**: 101–106
- Suzuki H, Fujioka S, Takatsuto S, Yokota T, Murofushi N, Sakurai A** (1994a) Biosynthesis of brassinolide from teasterone via typhasterol and castasterone in cultured cells of *Catharanthus roseus*. *J Plant Growth Regul* **13**: 21–26
- Suzuki H, Inoue T, Fujioka S, Takatsuto S, Yanagisawa T, Yokota T, Murofushi N, Sakurai A** (1994b) Possible involvement of 3-dehydroteasterone in the conversion of teasterone to typhasterol in cultured cells of *Catharanthus roseus*. *Biosci Biotechnol Biochem* **58**: 1186–1188
- Swaczynova J, Novak O, Hauserova E, Fuksova K, Sisa M, Kohout L, Strnad M** (2007) New techniques for the estimation of naturally occurring brassinosteroids. *J Plant Growth Regul* **26**: 1–14
- Szekeres M, Németh K, Koncz-Kálmán Z, Mathur J, Kauschmann A, Altmann T, Rédei GP, Nagy F, Schell J, Koncz C** (1996) Brassinosteroids rescue the deficiency of CYP90, a cytochrome P450, controlling cell elongation and de-etiolation in *Arabidopsis*. *Cell* **85**: 171–182
- Tanabe S, Ashikari M, Fujioka S, Takatsuto S, Yoshida S, Yano M, Yoshimura A, Kitano H, Matsuoka M, Fujisawa Y, et al** (2005) A novel cytochrome P450 is implicated in brassinosteroid biosynthesis via the characterization of a rice dwarf mutant, *dwarf11*, with reduced seed length. *Plant Cell* **17**: 776–790
- Wang KL, Li H, Ecker JR** (2002a) Ethylene biosynthesis and signaling networks. *Plant Cell (Suppl)* **14**: S131–S151
- Wang X, Chory J** (2006) Brassinosteroids regulate dissociation of BKI1, a negative regulator of BRI1 signaling, from the plasma membrane. *Science* **313**: 1118–1122
- Wang ZY, Nakano T, Gendron J, He J, Chen M, Vafeados D, Yang Y, Fujioka S, Yoshida S, Asami T, et al** (2002b) Nuclear-localized BZR1 mediates brassinosteroid-induced growth and feedback suppression of brassinosteroid biosynthesis. *Dev Cell* **2**: 505–513
- Yanagisawa S** (2002) The Dof family of plant transcription factors. *Trends Plant Sci* **7**: 555–560
- Yanagisawa S** (2004) Dof domain proteins: plant-specific transcription factors associated with diverse phenomena unique to plants. *Plant Cell Physiol* **45**: 386–391
- Yang YZ, Tan BC** (2014) A distal ABA responsive element in *AtNCED3* promoter is required for positive feedback regulation of ABA biosynthesis in *Arabidopsis*. *PLoS ONE* **9**: e87283
- Yin Y, Wang ZY, Mora-García S, Li J, Yoshida S, Asami T, Chory J** (2002) BES1 accumulates in the nucleus in response to brassinosteroids to regulate gene expression and promote stem elongation. *Cell* **109**: 181–191
- Yokota T, Ogino Y, Takahashi N, Saimoto H, Fujioka S, Sakurai A** (1990) Brassinolide is biosynthesized from castasterone in *Catharanthus roseus* crown gall cells. *Agric Biol Chem* **54**: 1107–1108
- Yu X, Li L, Zola J, Aluru M, Ye H, Foudree A, Guo H, Anderson S, Aluru S, Liu P, et al** (2011) A brassinosteroid transcriptional network revealed by genome-wide identification of BES1 target genes in *Arabidopsis thaliana*. *Plant J* **65**: 634–646
- Yuan T, Fujioka S, Takatsuto S, Matsumoto S, Gou X, He K, Russell SD, Li J** (2007) *BEN1*, a gene encoding a dihydroflavonol 4-reductase (DFR)-like protein, regulates the levels of brassinosteroids in *Arabidopsis thaliana*. *Plant J* **51**: 220–233
- Zhao B, Li J** (2012) Regulation of brassinosteroid biosynthesis and inactivation. *J Integr Plant Biol* **54**: 746–759
- Zhou A, Wang H, Walker JC, Li J** (2004) BRL1, a leucine-rich repeat receptor-like protein kinase, is functionally redundant with BRI1 in regulating *Arabidopsis* brassinosteroid signaling. *Plant J* **40**: 399–409